JOURNAL OF APPLIED ELECTROCHEMISTRY 22 (1992) 620–627

Cycling behaviour of lithium–aluminium alloys formed on various aluminium substrates as negative electrodes in secondary lithium cells

N. KUMAGAI, Y. KIKUCHI, K. TANNO

Department of Applied Chemistry, Faculty of Engineering, Iwate University, Morioka, 020, Japan

Received 22 January 1991; revised 18 June 1991

The cycling efficiencies of lithium were examined on various metal substrates using different methods. The efficiency was found to be strongly dependent on the evaluating method and on the alloying process of lithium with the metal substrates. The electrochemical behaviour of the Li–Al alloys formed on several kinds of thin Al substrates were investigated in 1 M propylene carbonate solution of $LiClO_4$ at room temperature. It was found that the cycling behaviour was dependent on the alloying rate of lithium with the Al substrate, and the electrochemically etched Al substrate, having a microstructure of a considerably preferred (1 0 0) orientation and a larger effective surface area, gave excellent cycling behaviour, showing a high cycling efficiency of 90 $\sim$ 85% at a high current density of $\sim 7\,mA\,cm^{-2}$.

1. Introduction

It is well known that there is considerable difficulty in obtaining high cycling efficiencies for lithium as a negative electrode in secondary lithium cells because of the dendritic nature of the electrodeposited metal and the formation of a passive film [1, 2]. For this reason, the use of Li–alloys is of considerable interest as an alternative electrode to pure lithium in secondary lithium cells operating at ambient temperatures [3, 4].

Electrochemical formation of a large number of lithium alloys of intermetallics in organic electrolytes has been demonstrated by Dey [5], and several electrochemical studies of Li–Al alloys in liquid organic electrolytes have subsequently been reported [6–12]. Recently the possibility of utilizing a thin aluminium substrate as a secondary Al–Li electrode has been demonstrated by Maskell and Owen [13], and furthermore the effect of thermal treatment of the foil on the electrochemical behaviour has been studied by Zlatilova *et al.* [14].

In the present work, the cycling efficiencies of lithium were examined on various metal substrates using different methods. The electrochemical behaviour of the Li–Al alloys formed electrochemically on thin aluminium substrates having different crystallinities and on electrochemically etched Al substrates were then investigated in an organic electrolyte. The morphology of the Li–Al alloys formed on the aluminium substrates was also examined by scanning electron spectroscopy (SEM).

2. Experimental details

2.1. *Materials, electrodes and cells*

The materials for the substrates were Ni (purity: 99.7%, thickness: 0.5 mm), Cu (99.9%, 0.5 mm), Zn (99.09%, 0.5 mm), Pb (99.28%, 0.25 mm), SUS 304 stainless steel (0.066%/C, 8.75%/Cr, 0.14%/Mo, 0.58%/Si, balance/Fe, 2.0 mm) and two kinds of Al, Al(LPC) (99.5%, 0.5 mm) and Al(POC) (99.8%, 0.1 mm)*, all obtained from Nilaco Co, and another kind of Al, Al(SAL) (99.99%, 0.1 mm)*, and three kinds of etched Al, etched Al(KH) (99.99%, 0.1 mm), etched Al(SL) (99.98%, 0.1 mm) and etched Al(TL) (99.8%, 0.1 mm), obtained from KDK Co. Preparation of these etched aluminium substrates is summarized in Table 1 and the SEM photographs are given in Fig. 13. The parent material for the etching treatment was Al(SAL).

The working electrodes were rectangular pieces with an exposed geometric area of $2.0\,cm^2$. As a pretreatment of the metal electrode surface, mechanical polishing or preplating with a small amount of lithium was performed. In the former treatment, the last finish was carried out with emery paper grade 6/0 in a glove dry box filled with an argon. The electrode was then rinsed with ethanol and dried. In the latter treatment, which was applied only for the aluminium substrate, the substrate was washed with ethanol, dried, and plated with $0.075\,C\,cm^{-2}$ lithium at a constant current density of $2.5\,mA\,cm^{-2}$, followed by standing for 30 min.

* From the X-ray diffraction measurement using a Cu$K\alpha$ line (Fig. 12), the intensity ratios of the (2 0 0) peak (2θ = 44.5°) of Al(LPC), Al(POC) and Al(KH) to Al(SAL) were 0.022, 0.11 and 1.3, respectively, which indicated that Al(SAL) and Al(KH) had a considerably preferred (1 0 0) orientation.

0021-891X/92

Table 1. Preparation of electrochemically etched aluminium substrates

Substrate	*Preparation*
Al(KH)	After etching with d.c., acid treatment with conc. HNO_3 (67%) at 40° C for 2 min
Al(SL)	After etching with a.c., treatment with 7%HNO_3 at 50° C and heat-treatment in air at 400° C for 25 h
Al(TL)	After etching with a.c., treatment with conc. phosphoric acid and heat-treatment in air at 400° C for 20 s

D.c. – direct current; a.c. – alternate current

Cell assembly and preparations of counter and reference electrodes and the electrolyte were carried out as described in previous papers [15, 16]. Both counter and reference electrodes were lithium pellets pressed on to nickel nets. The electrolyte used was 1.0 M $LiClO_4$–propylene carbonate(PC) obtained from Tomiyama Kagaku Chemicals, which contained only trace amounts of water, less than 20 mg dm^{-3}. The working electrode was wrapped with a non-woven polypropylene sheet and was further sandwiched between two counter electrodes (19 mm diameter, ~ 1.5 mm thickness). The distance between the working and counter electrodes was fixed at 5 mm by using a PTFE plunger. The element was then inserted into a cell case of a glass-beaker type and the cell was filled with approximately 20 ml of electrolyte solution. All the measurements and handling were carried out in a dry box filled with argon.

2.2. *Electrochemical measurements*

The following two different methods for estimating the charge/discharge cycling efficiency of lithium on various metal substrates were used. Plating and stripping were performed galvanostatically at 25° C by using an automatic cycling apparatus, and the repeated cycles were terminated automatically.

2.2.1. Average efficiency per cycle; $\bar{E}_a$ [17]. A known charge (Q_{init}), typically 4.8 C cm^{-2}, was used to plate the lithium at a constant current density (0.2 ~ 7 mA cm^{-2}) on to metal substrates, followed by standing for 30 min. Then a lower charge (Q_{cy}), typically 1.2 C cm^{-2}, was sequentially used to strip from and plate to the original substrate with a standing time of 30 min between them. After the first 1.2 C cm^{-2} strip, a 3.6 C cm^{-2} reservoir of excess lithium remained. Were each cycle 100% efficient, the cell would cycle indefinitely with a 3.6 C cm^{-2} reserve of lithium (efficiency = Q stripped/Q plated). Of course, each stripping cycle is < 100% efficient which means that each strip cuts into the lithium reserve yielding an apparent '100%' cycle until the substrate is reached. At this point the excess lithium is exhausted. In practice, when the stripping potential started to rise sharply above 2.0 V against Li/Li^+, the cycles were terminated.

The average efficiency per cycle, $\bar{E}_a$, was calculated according to

$$\bar{E}_a = \left(\frac{Q_{cy} - Q_{init}/n}{Q_{cy}}\right) \times 100\% \quad (1)$$

where n is the number of '100%' cycles.

2.2.2. Coulombic efficiency at each cycle, E_c [18]. A known charge (0.6 C cm^{-2}) was used to plate and strip lithium at a constant current density (0.5 mA cm^{-2}). The stripping was performed below the potential of 2.0 V against Li/Li^+. This cycle was repeated with a rest time of 30 min between the plating and stripping.

The coulombic efficiency was obtained at each cycle with

$$E_c = (Q_s/Q_p) \times 100\% \quad (2)$$

where Q_s and Q_p are the charge of lithium stripped and plated, respectively.

A.c. impedance measurements of the electrode were carried out in the frequency range 10^{+5}–10^{-3} Hz using a frequency response analyser (NF Electronic Instrument 5720B). The a.c. signal amplitude to the electrode was 5 mV. Scanning electron microscopy was carried out on an ALPHA-10 machine (Akashi Ltd).

3. Results and discussion

3.1. *Charge/discharge cycling efficiency of lithium on various metal substrates*

Several methods for estimating the cycling efficiency of lithium have been reported [9, 11, 17, 18]. According to these reports, the cycling efficiency depends on the method used; therefore two different methods as described in the experimental section, were used here. The average efficiencies of lithium per cycle, $\bar{E}_a$, obtained on various metal substrates, are given in Table 2. The lithium alloying metals such as aluminium and lead [5] were found to show higher $\bar{E}_a$ values, whereas non-alloying metals such as nickel, copper and stainless steel [5] showed $\bar{E}_a$ values of 67 to 71%. But, another lithium alloying metal, zinc, [5] showed nearly zero efficiency. The reason for this is discussed below. In Fig. 1, the coulombic efficiencies, E_c, obtained on different substrates are given as a function of the cycling number. This result also shows

Table 2. Average efficiencies, $\bar{E}_a$, for cycling of lithium on different metal substrates

Substrate	$\bar{E}_a$ (%)
Ni	71.1
Cu	66.7
Pb	83.3
Zn	0
Stainless steel (SUS 304)	66.7
Al(LPC)	90.0

c.d. = 0.5 mA cm^{-2}; Q_{init} = 2.7 C cm^{-2}; Q_{cy} = 1.8 C cm^{-2}

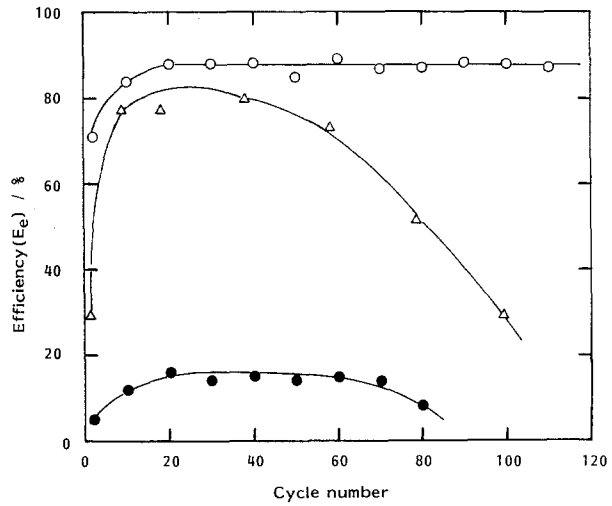

Fig. 1. Variations of coulombic efficiency, E_c, for cycling of Li on different metal substrates with cycle number. $Q_p = Q_s = 0.6\,C\,cm^{-2}$; $i_{cy} = 0.5\,mA\,cm^{-2}$. (○) Al(LPC), (●) Ni and (△) Zn.

that the alloying metal aluminium shows a higher efficiency than the non-alloying metal nickel. The results obtained from the two different methods indicate that aluminium substrate shows the highest efficiency among the metal substrates tested, which is in good agreement with previous work [1, 6, 7]. It was also found that aluminium substrate shows almost the same value for the two methods, while other substrates such as nickel and zinc show considerably different values for the two methods.

The SEM photographs of nickel and zinc substrates before and after electrodeposition of lithium are given in Fig. 2. A dendritic deposit of lithium was observed on the nickel substrate. On the zinc substrate after deposition of $4.8\,C\,cm^{-2}$ Li, however, there was hardly any deposit on the surface, indicating that all the lithium deposited may have been incorporated into the substrate. X-ray diffraction measurement of the zinc substrate before and after $2.4 \sim 4.8\,C\,cm^{-2}$ Li deposition (Fig. 3) revealed that the zinc substrate was alloyed by the deposition of lithium and the amount of Li–Zn alloy increased with increasing deposited lithium [19]. The overpotential for lithium stripping from the Li–Zn alloy increased considerably with stripping, resulting in a very low average efficiency, $\bar{E}_a$. These observations show that the differences in the efficiency may be due to the lithium alloying process as well as the evaluating method itself. From the above results, the average efficiency, $\bar{E}_a$, will be used for assessing the cycling efficiency of lithium on aluminium substrates in further work.

3.2. *Charge/discharge cycling efficiency of lithium on various aluminium substrates*

The mechanical polishing of aluminium substrates as a pre-treatment to remove the surface oxides may lead to disintegration of the pitting structure in the etched aluminium foil. Hence, other pre-treatments to remove the surface oxide have to be used. Here, preplating was tried prior to the cycling experiments. This treatment is based on the idea that the oxides on the surface and inside the pit can be reduced through the preplating and that a small amount of Li–Al alloy formed during the preplating may serve as a nucleus for further alloy formation. In Fig. 4 average cycling efficiencies,

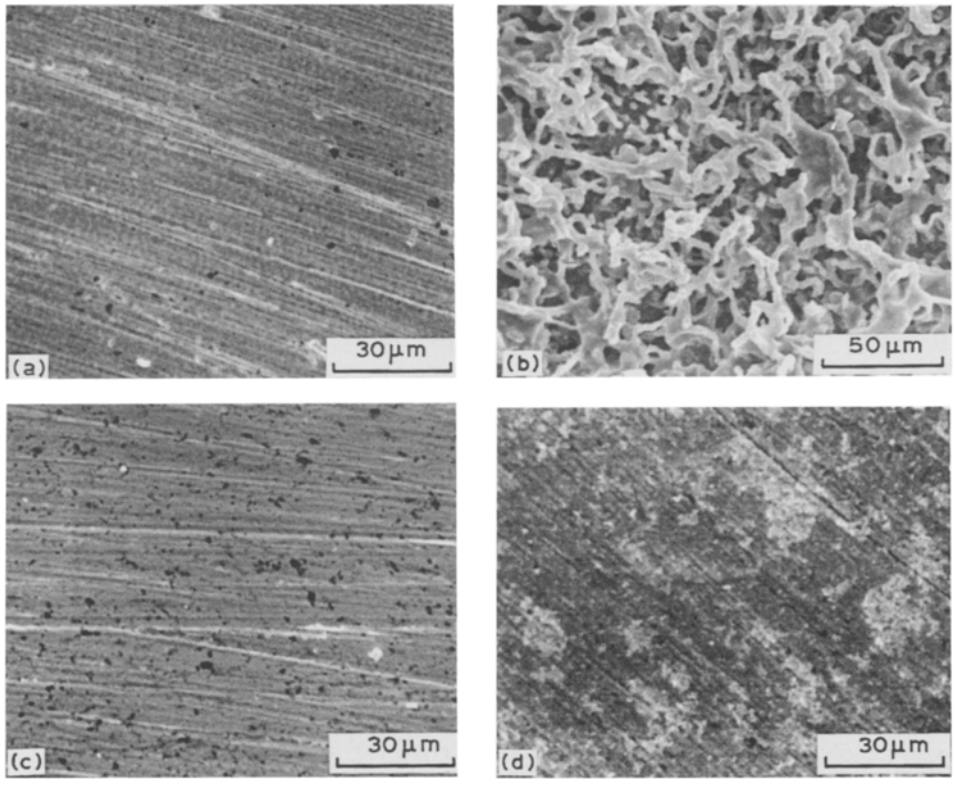

Fig. 2. SEM photographs of Ni and Zn substrates before and after plating. (a) Ni substrate before plating, (b) Ni substrate after plating $4.8\,C\,cm^{-2}$ Li at $2\,mA\,cm^{-2}$, (c) Zn substrate before plating, and (d) Zn substrate after plating $4.8\,C\,cm^{-2}$ Li at $2\,mA\,cm^{-2}$.

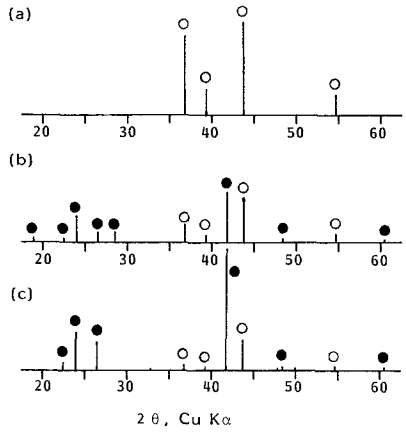

Fig. 3. X-ray diffraction patterns of Zn substrate before and after Li plating. (a) before plating, (b) after plating 2.4 C cm^{-2} Li at 2 mA cm^{-2}, (c) after plating 4.8 C cm^{-2} Li at 2 mA cm^{-2}. (○) Zn and (●) Li–Zn alloy.

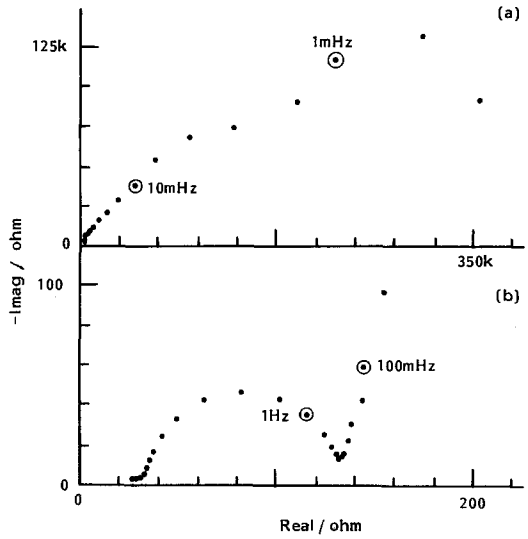

Fig. 5. Typical impedance diagrams of Al(LPC) substrate before and after preplating. (a) before preplating, (b) after preplating (0.75 C cm^{-2} Li at 2.5 mA cm^{-2}).

$\bar{E}_a$, obtained on the aluminium substrates with different kinds of pre-treatment, are given as a function of a current density. As can be seen from the figure, the preplated substrate showed considerably higher efficiency than that of the original substrate and had a somewhat higher $\bar{E}_a$ value, compared to the polished value. This result indicates that the preplating procedure is sufficiently effective as a surface pre-treatment. The SEM photographs of the aluminium substrates before and after preplating are given in Figs. 10a and b. As observed in the photographs, a smooth new product, which was probably a Li–Al alloy, was formed on the surface of the substrate. The formation of such a surface product may modify the interface between the electrolyte and the electrode through which lithium is inserted into the substrate. In order to examine the interface resistance of the lithium insertion reaction, the a.c. impedance was measured on the aluminium substrates before and after preplating. The a.c. impedance diagrams obtained are given in Fig. 5. As the arc seen in the impedance plots is assumed to express a charge transfer process, the charge transfer resistance (R_{ct}) of lithium deposition on the substrate without preplating was about 400 kΩ, while on the substrate after preplating R_{ct} decreased significantly to ~ 100 Ω. Moreover, on the latter substrate a low-frequency spike, probably due to a finite length diffusion process, was observed after the high frequency charge–transfer arc [20]. Thus the formation of a new surface layer resulted in a significant decrease in the interface resistance R_{ct}.

The electrochemical behaviour of lithium deposited on the three kinds of thin aluminium substrate Al(POC), Al(SAL) and the etched Al(KH) were examined. For all these substrates preplatings were carried out as a pre-treatment. Typical potential changes during plating and stripping at a current of 2 mA cm^{-2} are given in Fig. 6. As seen in the figure, the potential of initial plating for Al(POC) (c) was constant at about − 100 mV against Li/Li$^+$ and then the potential increased rapidly with standing. This shows that free lithium was deposited on the substrate by initial plat-

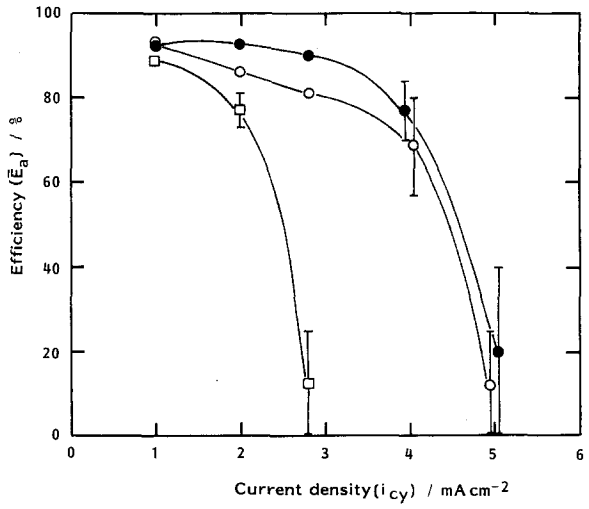

Fig. 4. Variations of average efficiency, $\bar{E}_a$, for cycling of Li on Al(LPC) substrate after different surface treatments as a function of a current density. Q_{init} = 4.8 C cm^{-2}; Q_{cy} = 1.2 C cm^{-2}; i_{init} = i_{cy}. (●) Preplating, (○) polishing and (□) without pre-treatment.

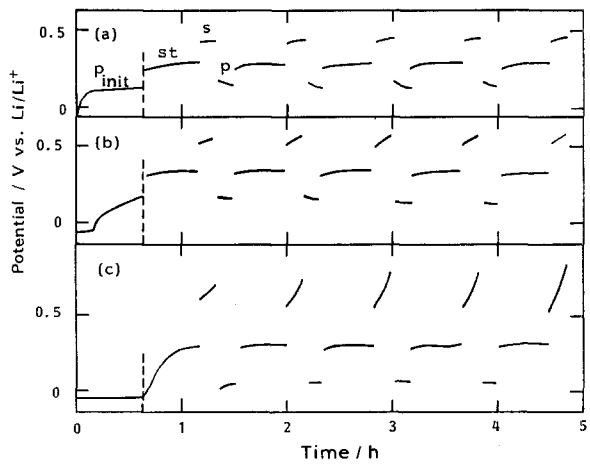

Fig. 6. Typical potential changes for cycling of Li on some Al substrates. (a) etched Al(KH), (b) Al(SAL) (c) Al(POC), current density: 2 mA cm^{-2}. Q_{init} = 4.8 C cm^{-2}; Q_{cy} = 1.2 C cm^{-2}; P_{init}: initial plating, st: standing, s: stripping, p: plating.

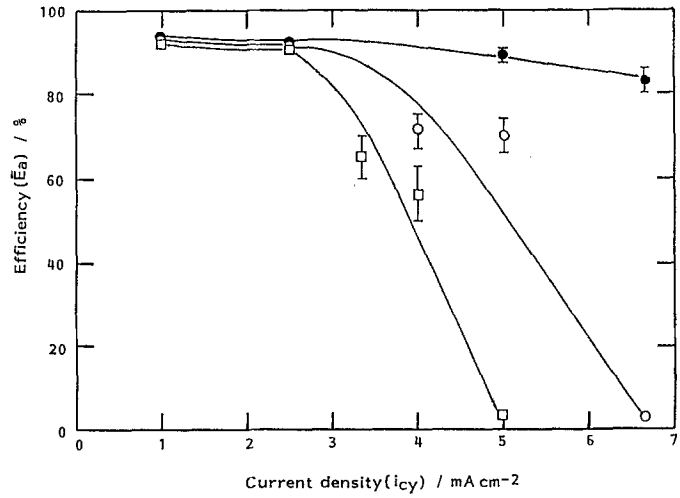

Fig. 7. Variations of efficiency, $\bar{E}_a$, for cycling of Li on some Al substrates as a function of a current density. $Q_{init} = 4.8\,C\,cm^{-2}$; $Q_{cy} = 1.2\,C\,cm^{-2}$; $i_{init} = i_{cy}$. (●) etched Al(KH), (○) Al(SAL) and (□) Al(POC).

ing and then the lithium diffused into the substrate to form a Li–Al alloy on standing [3, 10]. On the other hand, the potential of Al(SAL) (b) rose gradually during the initial plating and that for the etched Al(KH) (a) rose rapidly at the very beginning of the plating. Such potential changes with initial plating and standing are directly related to the alloying rate of lithium with the aluminium substrate. These results indicate that the alloying rate may be in the following order: the etched Al(KH) > Al(SAL) > Al(POC). Furthermore, it was observed that the stripping potentials during successive cyclings increased in the reverse order. The average cycling efficiency, $\bar{E}_a$, for the three kinds of aluminium substrate are given in Fig. 7 as a function of current density. Preplatings were carried out prior to all the tests. The etched Al(KH), which has a larger surface area, gave considerably higher efficiency, above 80%, even at higher current density of about 7 mA cm^{-2} than the parent Al(SAL). Furthermore, it was found that the Al(SAL), which had a more preferred (1 0 0) orientation, gave higher efficiency than Al(LPC) and Al(POC) (Figs. 4 and 7). Cyclic voltammograms of a lithium electrode on the Al substrates are shown in Fig. 8. Preplatings with a smaller amount of lithium (0.02 C cm^{-2} at 2.5 mA cm^{-2}) were carried out as a pre-treatment prior to the voltammetric measurements. As can be see in the figure, two anodic peaks I and II appeared. Peak I was due to the dissolution of free lithium on the substrate and peak II was due to the anodic dissolution of lithium from the Li–Al alloy [7]. On the Al(POC) (a), peak II remained almost unchanged during 5 cyclings. On the other hand, on the Al(SAL) with a higher crystallinity, it is noted that peak II increased with increasing cycle number. Furthermore, on the etched aluminium, peak II appeared almost alone, increasing with increasing cycle number. This shows that almost all the deposited lithium was alloyed on the etched aluminium, whereas a part of the deposited lithium was alloyed on the other aluminium substrates without etching. Moreover, it was found that alloying of lithium on the Al(SAL) proceeded more rapidly than that on Al(POC), probably leading to the higher cycling efficiency. The voltammetric results are consistent with those from galvanostatic measurements (Fig. 6). Thus the cycling efficiency, $\bar{E}_a$, can be related to the rate of lithium alloying with the aluminium substrate.

Charge/discharge cyclings of lithium were carried out on some etched aluminium substrates. Preplatings were performed as a pre-treatment. $\bar{E}_a$ values obtained are given at two different current densities, compared with the value on the parent Al(SAL) (Table 3). All the etched aluminium substrates showed high $\bar{E}_a$ values of about 82 ~ 92% at a lower current density of 0.5 mA cm^{-2}. At a higher current density of 5 mA cm^{-2}, however, the $\bar{E}_a$ values were considerably different in each substrate; Al(KH) gave the highest value of about ~90% and Al(TL) gave a value close to the parent Al(SAL), whereas the value of Al(SL)

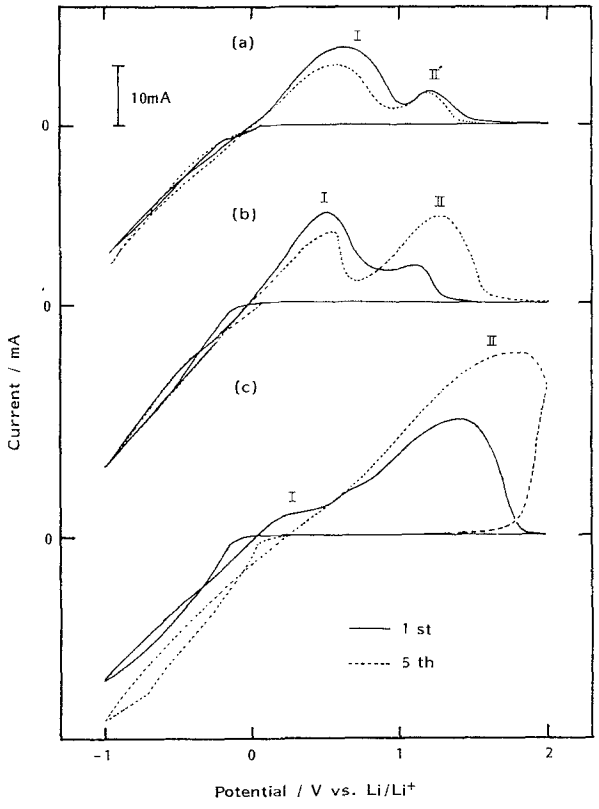

Fig. 8. Cyclic voltammograms on some Al substrates. (a) Al(POC), (b) Al(SAL), (c) etched Al(KH). Surface area = 2.0 cm^2, Sweep rate: 10 mV s^{-1}

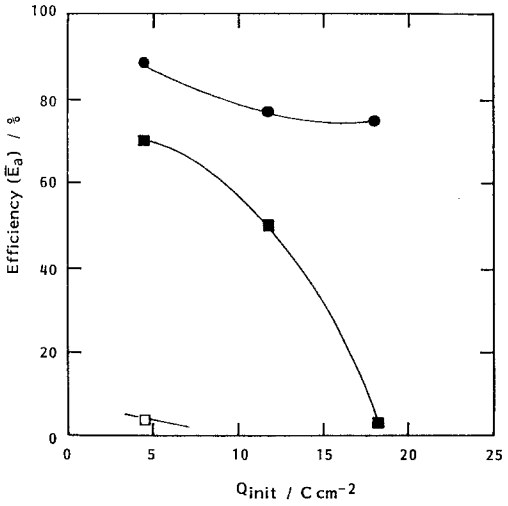

Fig. 9. Variations of average efficiency, $\bar{E}_a$, with a charge for initial plating. Q_{init}: $Q_{cy} = 4:1$, $i_{init} = i_{cy} = 5\,mA\,cm^{-2}$. (●) etched Al(KH), (■) Al(SAL) and (□) Al(POC).

fell to 0%. This result may be related to the amount of surface compounds such as oxide and phosphate (Table 1). Particularly, in the case of Al(SL) the surface and pits in the substrate were found to be mostly covered with a thick oxide layer by SEM observation (Fig. 13d). This surface oxide would block the lithium insertion into the bulk substrate. The cycling efficiency, $\bar{E}_a$, for the three kinds of thin aluminium substrates are given in Fig. 9 as a function of Q_{init}. These measurements were carried out at a constant ratio of $Q_{init}:Q_{cy} = 4:1$ and at a current density of $5\,mA\,cm^{-2}$. The efficiency in Al(SAL) decreased considerably with increasing Q_{init} and Q_{cy}. On the other hand, the etched Al(KH) showed higher efficiency of about 80% even at the Q_{init} of $18\,C\,cm^{-2}$ and $Q_{cy} = 4.5\,C\,cm^{-2}$, compared with the parent Al(SAL) and Al(POC). However, disintegration of the etched aluminium substrates occurred above $24\,C\,cm^{-2}$. This is a most likely cause of the considerable decrease in the $\bar{E}_a$ value.

3.3. *The morphology of the lithium layer formed on the aluminium substrate*

SEM photographs of the Al(LPC) substrates before and after lithium deposition are given in Fig. 10. At the initial stage of lithium deposition ($0.075\,C\,cm^{-2}$) (b), a smooth, alloyed surface was observed on the substrate, and the smooth, surface deposit appeared to grow on further deposition to $4.8\,C\,cm^{-2}$ at a low current density of $2\,mA\,cm^{-2}$ (c). At a higher current density of $5\,mA\,cm^{-2}$, however, a dendritic deposit probably composed of free lithium was observed (d).

Such a dendritic deposit was also seen on non-alloying metals such as Ni (Fig. 2). In this case the cycling efficiency, $\bar{E}_a$, decreased considerably, as seen in Fig. 4. From the SEM photographs and X-ray diffraction patterns of the lithium layer formed on the Al(SAL) with a microstructure of a preferred (1 0 0) orientation (Figs 11 and 12), a smooth, alloyed surface, with islands distributed on the surface of the substrate, was observed. The alloyed surface of the Al(SAL) giving the higher rate of Li alloying seemed to be smoother than that of Al(LPC). The cross-section (Fig. 11c) indicates that the Li–Al alloy layer was formed at the surface of the substrate and the

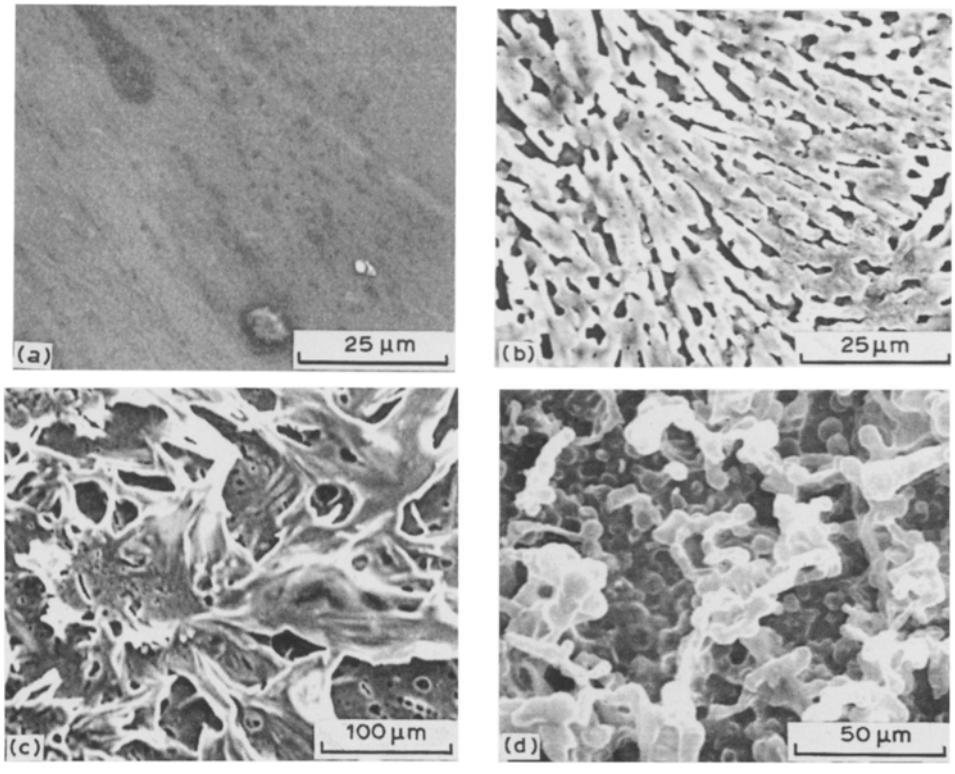

Fig. 10. SEM photographs of the surface of Al(LPC) substrate before and after plating. (a) before plating, (b) after preplating as a pretreatment ($0.075\,C\,cm^{-2}$ Li at $2.5\,mA\,cm^{-2}$), (c) after plating $4.8\,C\,cm^{-2}$ Li at $2\,mA\,cm^{-2}$, (d) after plating $4.8\,C\,cm^{-2}$ Li at $5\,mA\,cm^{-2}$.

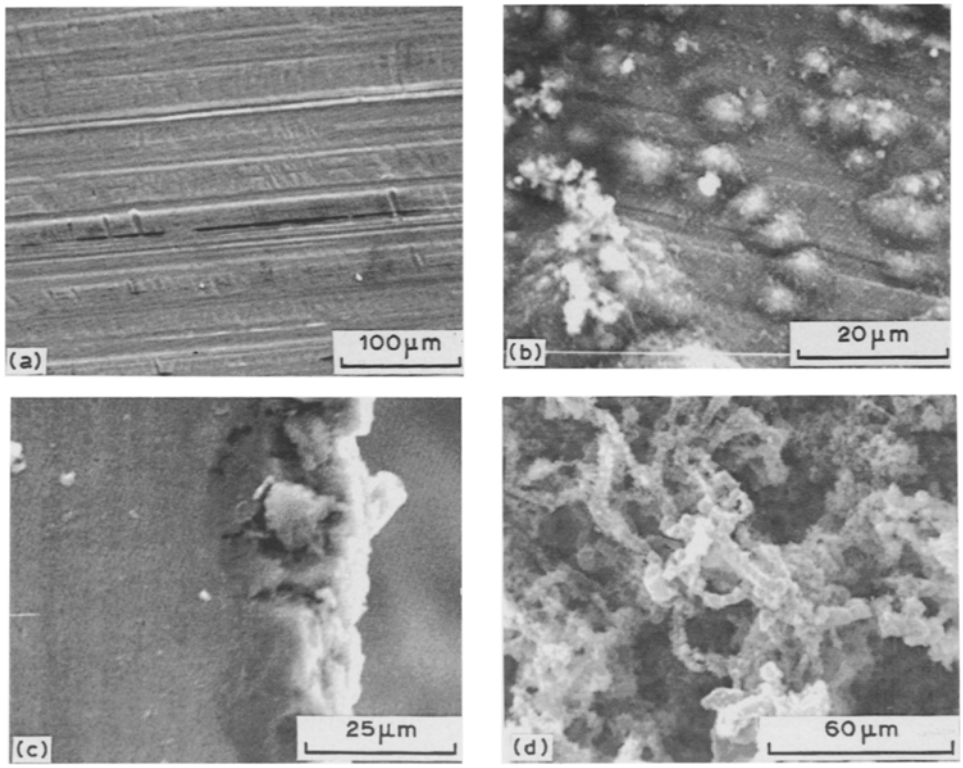

Fig. 11. SEM photographs of Al(SAL) before and after plating. (a) before plating, (b) after plating 4.8 C cm^{-2} Li at 2 mA cm^{-2}, (c) the cross section of (b), (d) after cycled to completion (Q_{init} = 4.8 C cm^{-2}, Q_{cy} = 1.2 C cm^{-2}, i_{cy} = 5.0 mA cm^{-2}).

thickness of the alloy layer was in the range 10–20 μm. Although the Li–Al alloy was formed at the surface of the substrate, the rate of lithium alloying depended on the crystalline structure of the aluminium bulk, and the Al(SAL) with a preferred (1 0 0) orientation showed a higher cycling efficiency. When cycling on the Al(SAL) substrate was performed at 5.0 mA cm^{-2} to completion (Fig. 11d), dendritic and powder-like deposits were observed. This shows that the cycling efficiency at a higher current density above 5 mA cm^{-2} (Fig. 7) decreased, probably because of mechanical degradation of the electrode. The X-ray diffraction patterns of the Al(SAL) before and after lithium deposition to 4.8 C cm^{-2} (Fig. 12) confirm the formation of a Li–AL alloy on the substrate [21]. The potential of the alloy, ~360 mV against Li/Li$^+$, indicates the formation of β-type Li–AL [3, 10]. A similar β-Li–AL was also observed on the other substrates such as Al(LPC), Al(POC) and Al(KH). When 4.8 C cm^{-2} lithium was deposited on the etched Al(KH), an alloyed layer was also observed on the surface, and the pitting structure was maintained during the deposition (Fig. 13). The volume expansion of the aluminium substrate due to a near doubling of molar volume is caused by the incorporation of lithium during the formation of the β-Li–Al phase. The pitting structure of the etched aluminium may absorb such a volume expansion and also gives a larger effective surface area for lithium incorporation. Thus, a smooth, thin Li–Al alloy is formed at the surface of the aluminium substrate,

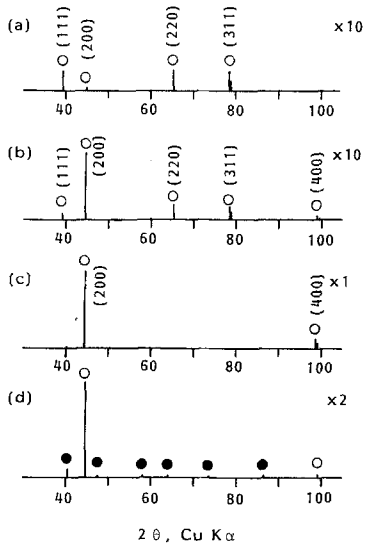

Fig. 12. X-ray diffraction patterns of various Al substrates and the Al(SAL) after Li plating. (a) Al(LPC), (b) Al(POC), (c) Al(SAL), (d) Al(SAL) after 4.8 C cm^{-2} Li plating at 2 mA cm^{-2}. Diffraction peaks are indexed by a cubic lattice.

Table 3. Average efficiencies, $\bar{E}_a$, for lithium cyclings on etched aluminium substrates at different current densities

Substrate	$\bar{E}_a$ (%)	
	at 0.5 mA cm^{-2}	*at 5 mA cm^{-2}*
Al(KH)	92.0	89.2
Al(SL)	81.8	0
Al(TL)	88.9	70.0
Al(SAL)	93.0	71.0

Q_{init} = 4.8 C cm^{-2}; Q_{cy} = 1.2 C cm^{-2}

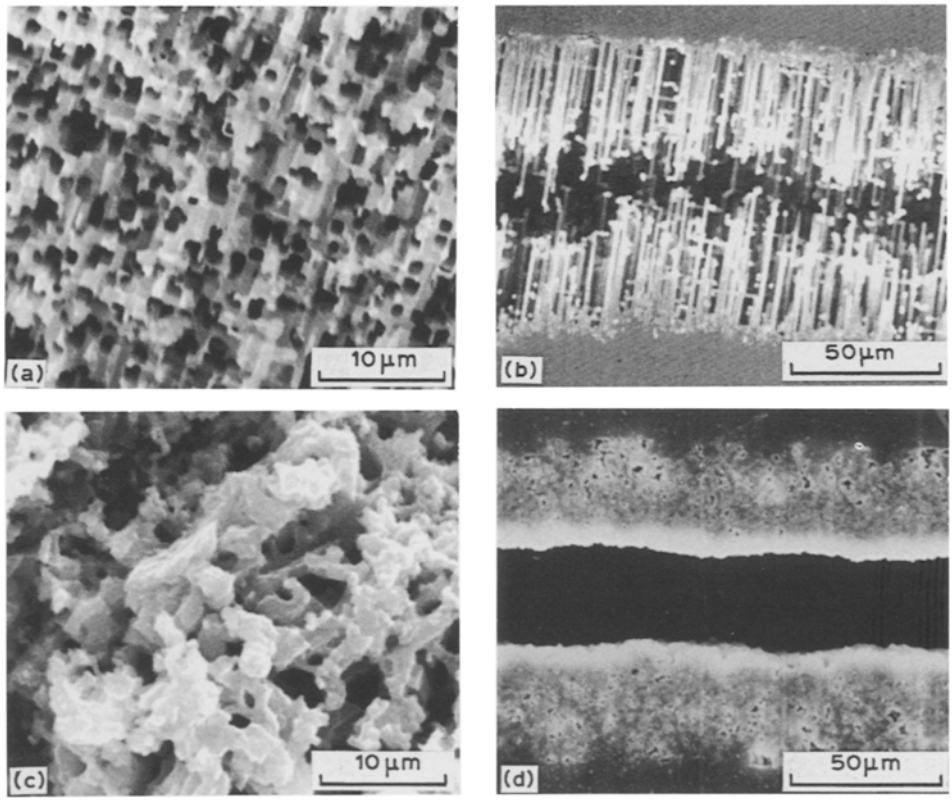

Fig. 13. SEM photographs of etched Al before and after plating (a) the surface of Al(KH), (b) the cross-section of Al(KH), (c) the surface of the Al(KH) after plating 4.8 C cm^{-2} Li at 2 mA cm^{-2}, (d) the cross-section of Al(SL). (b) and (d) are photographs of the surface oxide layer remaining after anodically dissoluting Al metal from the etched Al foil burried in an acryl resin in a Br_2–CH_3OH solution.

which may reduce the overpotential for lithium stripping from the alloy. Furthermore, the electrochemically etched Al(KH) having a considerably preferred (1 0 0) orientation and a larger effective surface area gave the high rate for lithium alloying and reduced the stripping overpotential of lithium from the surface Li–Al alloy, resulting in an excellent charge-discharge cycling behaviour of a Li–Al alloy.

Acknowledgement

The authors wish to express their thanks to Mrs Nobuko Kumagai, Mr S. Fujita and Mr Y. Sasaki for their helpful assistance in the experimental work, and also to KDK Co. for the provision of aluminium materials.

References

[1] J. O. Besenhand and G. Eichinger, *J. Electroanal. Chem.* **68** (1976) 1.
[2] V. R. Koch, *J. Power Sources* **6** (1981) 357.
[3] B. M. L. Rao, R. W. Francis and H. A. Christopher, *J. Electrochem. Soc.* **124** (1977) 1490.
[4] J. O. Besenhard, *J. Electroanal Chem.* **94** (1978) 77.
[5] A. N. Dey, *ibid.*, **118** (1971) 1557.
[6] I. Epelboin, M. Froment, M. Garreau, J. Thevenin and D. Warin, *J. Electrochem. Soc.* **127** (1980) 2100.
[7] Y. Takada, *Denki Kagaku* **49** (1981) 96.
[8] Y. Matzuda, M. Morita and H. Katzuma, *ibid.* **49** (1981) 537.
[9] A. S. Baranski and W. R. Fawcett, *J. Electrochem. Soc.* **129** (1982) 901.
[10] T. R. Jow and C. C. Liang, *ibid.*, **129** (1982) 1429.
[11] Y. Geronov, P. Zlatilova and R. V. Moshtev, *J. Power Sources* **12** (1984) 145.
[12] Y. Geronov, P. Zlatilova and G. Staikov, *ibid.*, **12** (1984) 155.
[13] W. C. Maskell and J. R. Owen, *J. Electrochem. Soc.* **132** (1985) 1602.
[14] P. Zlatilova, I. Balkanov and Y. Geronov, *J. Power Sources* **24** (1988) 71.
[15] N. Kumagai and K. Tanno, *Denki Kagaku* **48** (1980) 601.
[16] N. Kumagai, K. Tanno and N. Kumagai, *Electrochim. Acta* **27** (1982) 1087.
[17] R. D. Rauh, T. F. Reise and S. B. Brummer, *J. Electrochem. Soc.* **125** (1978) 186.
[18] V. R. Koch and S. B. Brummer, *Electrochim. Acta* **23** (1978) 55.
[19] ASTM card, 3–0954.
[20] C. Ho, I. D. Raistrick and R. A. Huggins, *J. Electrochem. Soc.* **127** (1980) 343.
[21] ASTM card, 3–1215.